

The friction of diamond sliding on diamond

B. SAMUELS*, J. WILKS

Clarendon Laboratory, Oxford, OX1 3PU, UK

Measurements are reported of the friction of diamond styli polished to a spherical tip sliding over a flat polished diamond surface. Particular attention was paid to maintaining standard conditions during the experiments, particularly the crystallographic orientations of the styli, the flat surface, and the directions of sliding, as well as the conditions of polish. The coefficient of friction was determined for sliding on both (001) and (011) faces, in different sliding directions, and for a range of loads and tip radii. The value of the friction and its variation with the direction of sliding depend quite strongly on the magnitude of the load and the radius of the stylus. However, the present results show that styli of different radii give quite similar friction when sliding under the same mean contact pressure. Hence, apparent discrepancies between previous measurements of the friction may be related to different regimes of pressure in the different experiments. When the stylus slides in the direction of easy abrasion of the flat the coefficient of friction passes through a pronounced minimum value as the contact pressure is increased. This behaviour suggests that at least two mechanisms contribute to the friction. A discussion based on the unusual topography of polished diamond surfaces, shows that the forces and energy losses associated with the friction may arise via at least three different mechanisms. The main features of the present results may be accounted for by two of these mechanisms in which surface asperities either ride over each other or push each other aside. (The third mechanism involving only fracture of the asperities appears to make no significant contribution.)

1. Introduction

Detailed measurements of the coefficient of friction of diamond sliding on diamond have been made by several workers, but a first sight their various results are not entirely consistent. For example, Enomoto and Tabor [1, 2] report that the coefficient rises with increasing load, Casey and Wilks [3] that it is independent of the load, and Hillebrecht [4] that it decreases slightly with increasing load. Equally, there has been no general agreement on the mechanism responsible for the friction. The present work was undertaken to extend and clarify experimental results and to elucidate the underlying mechanisms. Before describing this work it will be useful to summarize some of the more important of the earlier results.

Experiments have usually been made in air with some form of diamond stylus sliding over a polished (001) face, and lead to quite low values for the coefficient of friction of the order of 0.05 to 0.1. If the measurements are made in a high vacuum, the friction is greatly increased by about a factor of 10 [5], presumably because the surface are then free of films adsorbed from the atmosphere. However, the high vacuum condition is of no great practical interest so most experiments have been performed in air, with the surfaces covered with adsorbed layers. These layers are quite stable as demonstrated by Bowden and Hanwell [5] who observed that even in a moderately

high vacuum the adsorbed film was only removed after being subjected to several hundred passes of a stylus. Hence, it is assumed that the surfaces in all the present and similar previous experiments were covered by an adsorbed film of air.

One of the most interesting features of the friction observed by Seal [6] and others on polished (001) surfaces is that the coefficient of friction depends on the direction in which the stylus slides relative to the crystal axes of the flat surface. Quite commonly the friction is about twice as great in $\langle 100 \rangle$ directions as in $\langle 110 \rangle$ directions, even on apparently smooth and well polished faces. As might be expected, the friction on an (001) surface generally shows the four-fold symmetry of that face (Fig. 1a). However, if the same cube face is polished not in the usual manner by abrasion in $\langle 100 \rangle$ directions but in the more resistant $\langle 110 \rangle$ directions, the magnitude of the friction is changed (Fig. 1b) and shows only a two-fold symmetry.

The friction depends on the method of polishing the flat surface because the conventional polishing of diamond with diamond powder has some rather unusual features. As discussed elsewhere, material is removed by a chipping or cleavage process on a very fine scale of the order of 5 nm [7-9]. It follows that polishing in $\langle 100 \rangle$ directions will produce a topography with an overall four-fold symmetry, while a similar polish in $\langle 110 \rangle$ directions will produce

*Present address: Thornton Research Centre, P.O. Box 1, Chester, CH1 35H.

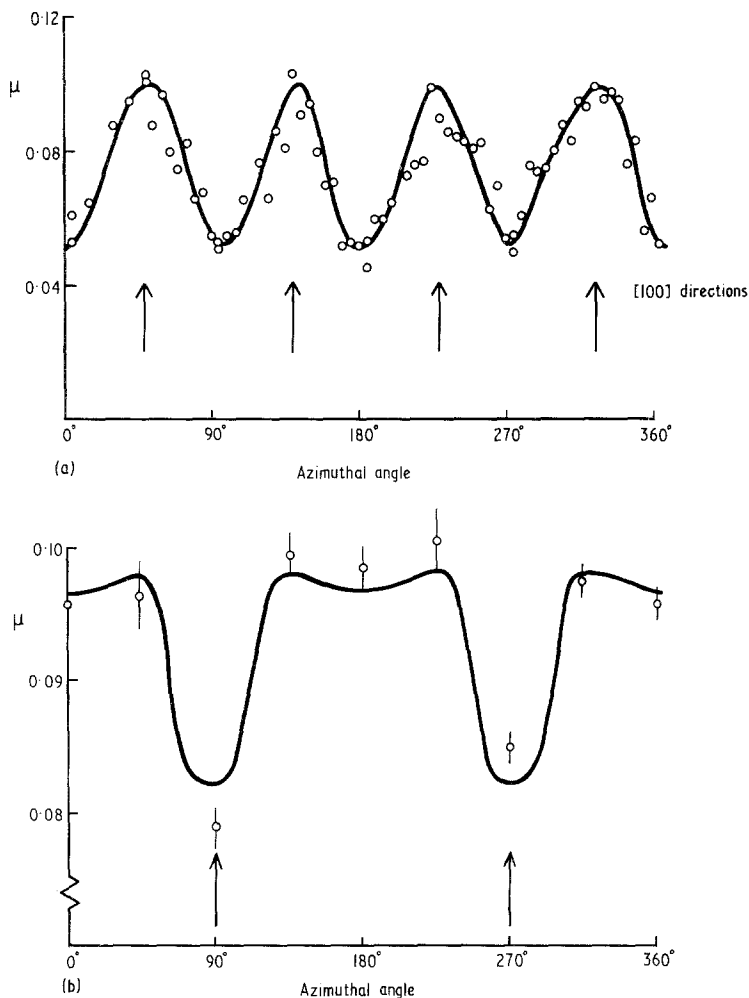


Figure 1 The coefficient of friction on an (001) surface as a function of sliding direction. The surface in Fig. 1a has been polished in the [100] direction and in Fig. 1b in the [110] direction (Casey and Wilks [3]).

a topography with only a two-fold symmetry [3]. This result implies that the magnitude of the friction is much affected by the topographical detail of the surface.

The importance of the surface topography is also shown by several other experiments. Thus a particularly smooth surface showing no sign of the usual polish lines may be obtained by a polishing process using oxidizing agents on a cast-iron scaife [10], and this treatment reduces the coefficient of friction by about a factor of 2 in all directions [11]. Another surface polished in the normal way and then further polished by the ion-beam technique exhibited coefficients of friction of about 0.15 which were essentially independent of the direction of sliding. Finally, Enomoto and Tabor [1, 2] have described how the presence of polishing lines may reduce the four-fold symmetry of the friction on a polished (001) face.

If the coefficient of friction is influenced by the microtopography of the flat surface, it will also depend on the microtopography of the stylus. However, it is difficult to fabricate and inspect styli, so their geometry and surface condition have often been rather ill-defined. Many of the styli used, although polished to a nominally spherical surface characterized by a measured radius, were of uncertain crystallographic orientation. Casey and Wilks [3] used the natural tips of octahedral diamonds, which permitted the styli to be crystallographically oriented with respect to the diamond flat and the direction of sliding. On the other hand, the use of the natural tips with their rather non-uniform geometry adds a further uncertainty into

the experiment. A particularly striking experiment was made by Bowden and Brookes [12] who measured the friction on (001) faces using cone-shaped styli with included angles of 60°, 120° and 170°. They found that the anisotropy of the friction was much more marked with the sharper styli (Fig. 2) and concluded that the wider ones were unable to follow the finer details of the surface topography.

The coefficient, μ , may also be influenced by the

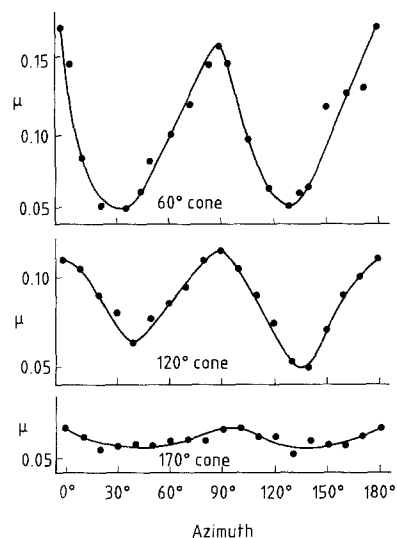


Figure 2 The coefficient of friction of three cones of different apex angle sliding on an (001) surface as a function of sliding direction (Bowden and Brookes [12]).

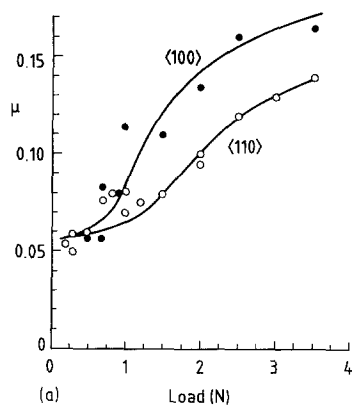
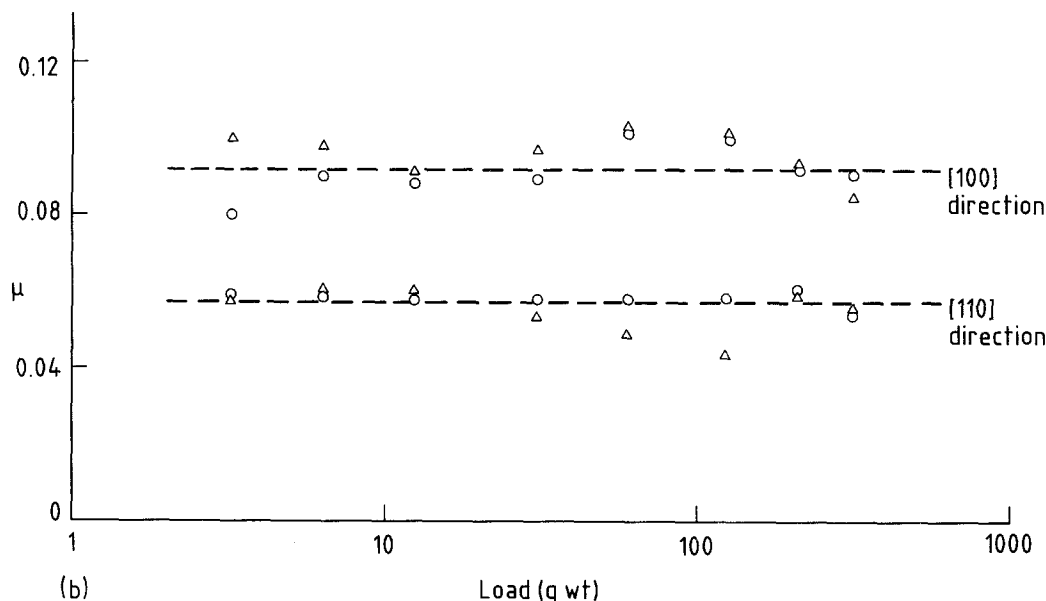


Figure 3 The friction of diamond sliding on (001) surfaces in $\langle 100 \rangle$ and $\langle 110 \rangle$ directions as a function of load. (a) Spherical stylus of radius $80 \mu\text{m}$ (Enomoto and Tabor [2]). (b) Tip of a natural octahedron diamond (Casey and Wilks [3]).



magnitude of the load on the stylus. For example, Enomoto and Tabor [2] using a rounded stylus obtained the results shown in Fig. 3a where μ increases with increasing load, and the anisotropy is almost zero for the lowest load, and increases as the load is increased. On the other hand, Casey and Wilks [3] using the tip of a natural octahedron found that μ was independent of the load, W , over a wide range of W (Fig. 3b). Then, differently again, Hillebrecht [4] using a rounded stylus observed a coefficient of friction which showed no anisotropy and tended to be less at higher loads.

A further complication is that the value of μ may be affected by the measurement itself. For example, Seal [13] describes experiments in which up to 10 000 passes were made over the same track and observed considerable modifications to the friction. In fact, the amount of change produced by a measurement is very dependent on the orientation of the stylus. For example, Casey [14] observed that with some orientations an appreciable change in μ occurred after only a few passes. Casey also observed that the magnitude of this effect varied with the direction of sliding.

The friction of diamond sliding on diamond is a complex phenomenon influenced by many parameters. Hence, it is difficult to compare and assess the results of all the various experiments. In particular, there are generally uncertainties concerning the shape and orientation of the stylus, the orientation of the flat, and the polish on both flat and stylus. Hence, the aim of the present experiments was to study the friction by

specifying as many parameters as possible and then observing how μ changes as the load on the stylus is varied, the other parameters being kept constant.

2. Experimental techniques

A general view of the apparatus is given in Fig. 4 and some details in Fig. 5. The principal feature is a vertical brass beam mounted on a central axle which can rotate in ball-bearing races. The upper end of this beam carries the diamond specimen mounted on two sets of cross-slides so that it can be accurately positioned. The beam also carries two small weights mounted on screw threads which may be moved to ensure that the beam assembly is accurately balanced about the axis. When so balanced an additional weight of 0.5 g placed on either end of the beam was sufficient to cause rotation.

The diamond stylus is mounted on the axis of a steel rod which slides vertically in a linear bearing which has very low friction but permits little sideways motion of the rod. Additional loads on the stylus, above the weight of the rod, are provided by additional masses affixed to the upper end of the rod. Note that the position of the bearing and rod is adjusted so that the axis of the rod passes through the axis of the main bearing to avoid the stylus producing any torque on the beam. Fig. 4 also shows the electric motor and lifting cord used to lower and raise the rod and stylus to and from the flat at a very slow rate in order to avoid any impact damage to the diamond surfaces.

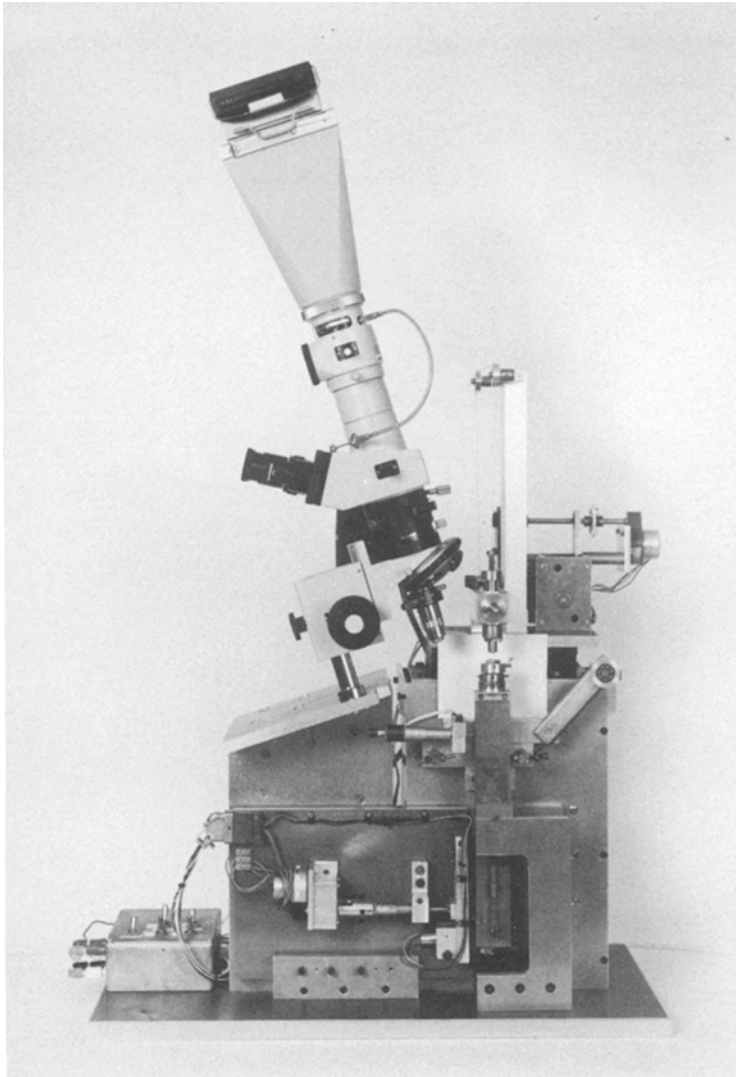


Figure 4 General view of the apparatus used to measure the friction.

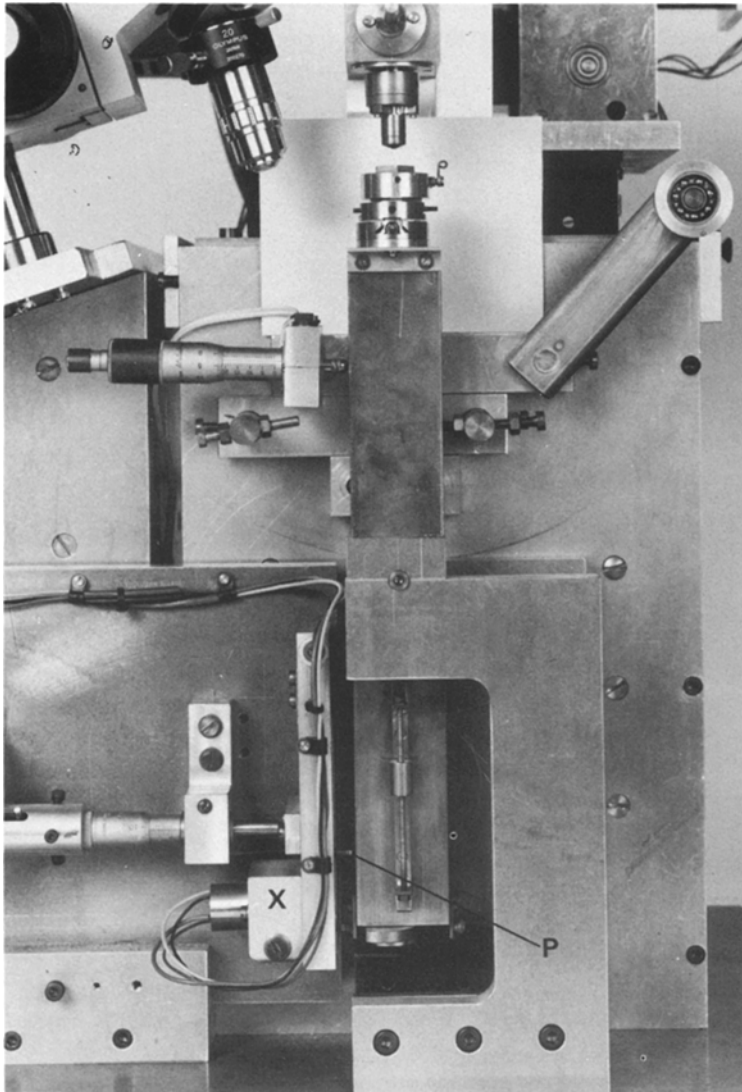
To perform an experiment, the beam is balanced and held upright against the upper micrometer and the stylus lowered on the flat. The micrometer stop is drawn back and a motor rotates the lower micrometer thus driving forward the assembly (X, Fig. 5) which pivots about an axis at its upper end. This assembly includes a spring plate carrying a pin (P, Fig. 5) which rotates the beam against the torque due to the friction between the diamonds. As the main beam rotates, the force on the pin, P, is determined by measuring the deflection of the spring plate using a linear displacement transducer whose output is fed to a chart recorder. To relate the deflection of the recorder to the actual friction force the apparatus is calibrated (with the stylus clear of the flat) by pulling the upper end of the beam to the right by a light cord, attached at the level of the flat, and passing over a pulley to a known weight. Thus, a calibration curve of friction force against chart deflection is obtained by observing the deflection for a range of weights.

The apparatus is designed for the stylus to carry maximum load of about 2 kg; the minimum load of 140 g is set by the weight of the rod and stylus. In contrast to earlier methods, the friction is measured by observing the force on the flat rather than on the loaded stylus. This arrangement removes the possibility that a distortion of the stylus suspension may

allow a direct component of the load to add directly to the much smaller friction force. The upper end of the beam may be swung to the left so that the diamond flat can be viewed in an optical microscope using the Nomarski interference technique. This arrangement allows the flat to be examined at any time and replaced in the same position, and also permits the precise positioning of the flat relative to the stylus.

Fig. 6 shows a typical set of recorder traces obtained during five successive passes on the track on a polished surface. The initial rapid rise occurs as the spring carrying the pin, P, comes under load. At the end of a pass this spring remains held in tension and the force is constant. During the pass the force fluctuates appreciably, presumably due to variations in the diamond surface, although the form of the traces is also determined by the mechanical response of the measuring system itself. We see that the value of the friction varies during a pass, and also varies from pass to pass. However, by taking the mean level of the force for five passes we obtain values of the friction on adjacent tracks that are in agreement with each other to about 5%. Therefore, our standard procedure has been to make five passes and take the average value as described. That is, we regard the fluctuations of the friction as secondary phenomena (which are considered in more detail in Section 6.5).

Figure 5 Detail of Fig. 4. see text.



3. The diamond styli and flats

In order to work with well-defined geometries, all the measurements were made with spherically tipped styli sliding over flat surfaces. Spherical styli were preferred both because the form of a spherical tip can be specified more precisely than, say, the tip of a conical slider, and because this shape reduces the possibility of any gouging into the flat. However, there is a complication in the use of spherical tips because as far as the friction is concerned the most relevant parameter may well be

the pressure between the surfaces rather than the total load. The well known Hertz relationships (see, for example, Johnson [15] p. 93) show that the mean pressure, p , over the area of contact varies only as $W^{1/3}$ where W is the applied load. Hence, in order to obtain a wide range of pressure, it was necessary to use several styli of radius, R , between 60 and 490 μm (the pressure being proportional to $1/R^{2/3}$).

Both styli and flats were polished on gem-quality colourless diamonds. Particular care was taken to

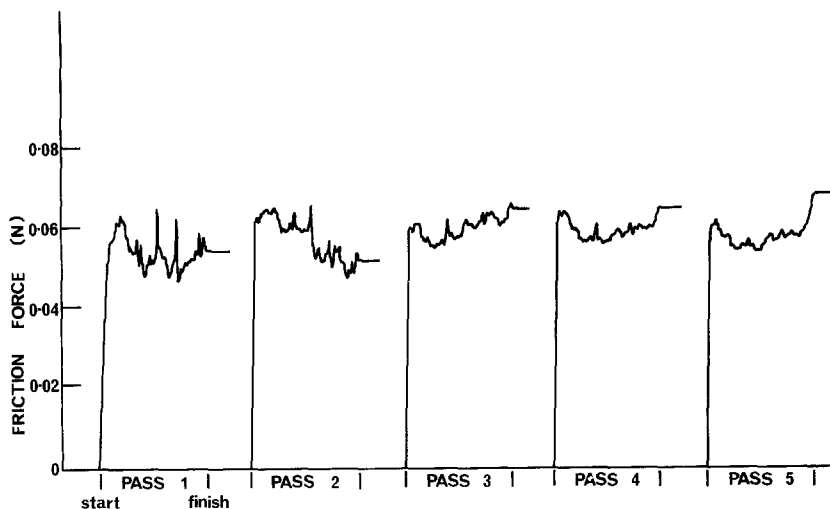


Figure 6 Typical chart recorder traces from five successive passes along the same track on an (001) surface. Radius of stylus 90 μm ; load 1.4 N; sliding direction [100].

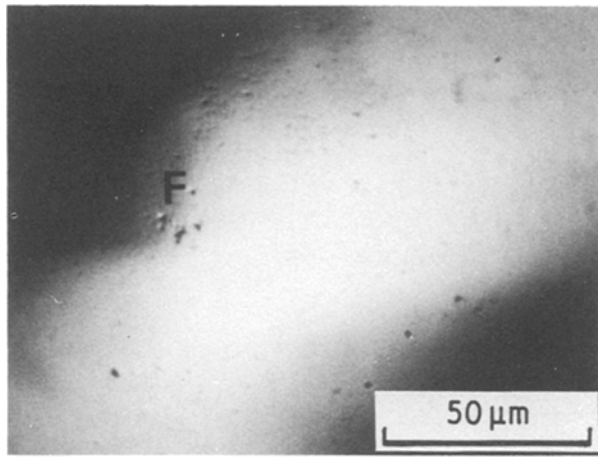


Figure 7 Optical Nomarski micrograph of the tip of a polished stylus of radius 340 μm .

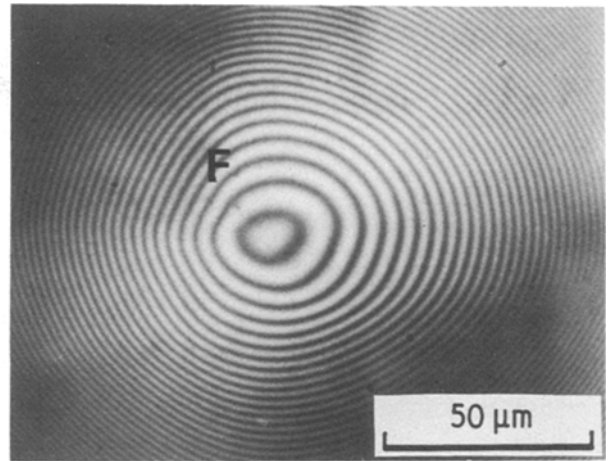


Figure 8 Newton's rings produced by the stylus of Fig. 7. The letter F marks a common feature.

establish their crystallographic orientation by using only diamonds with well-formed natural faces permitting their orientations to be determined by optical goniometry. Each stylus was fabricated by securing a natural octahedron to the end of a steel shank, and then machining the shank so that its axis was parallel to the $[110]$ axis of the diamond to within $15'$ of arc. The diamond was then polished to a spherical tip on a Habit Mark VI diamond lapping machine modified so that during polishing the diamond was swung about both horizontal and vertical axes, thus producing a central region quite closely spherical. The smoothest finish was obtained using a polishing wheel with $3\mu\text{m}$ diamond grit bonded in a metal matrix with the final polishing speed reduced to about 900 r.p.m.

Each polished stylus was examined after polishing to check that the surface was reasonably smooth when viewed in the optical microscope, and Fig. 7 shows the

appearance of a typical stylus. The radius and shape of the styli were checked and estimated by using Newton's rings (Fig 8). As mentioned above, the axis of all the styli was $[110]$. All were positioned so that the $[0\bar{1}1]$ axis was parallel to the direction of sliding. (The friction is known to depend on the orientation of the slider relative to the direction of sliding [13], and results are less complex when the stylus moves in its own most abrasion resistant direction [14].

The flat was either a (001) or (011) surface polished on a good quality colourless type I gem diamond with good octahedral faces suitable for optical goniometry. This diamond had also been selected because it gave a fairly uniform and bright background of luminescence when viewed in the cathodoluminescence mode (CL) of the scanning electron microscope. This made possible both the detection of any damage produced during a measurement, using the technique described

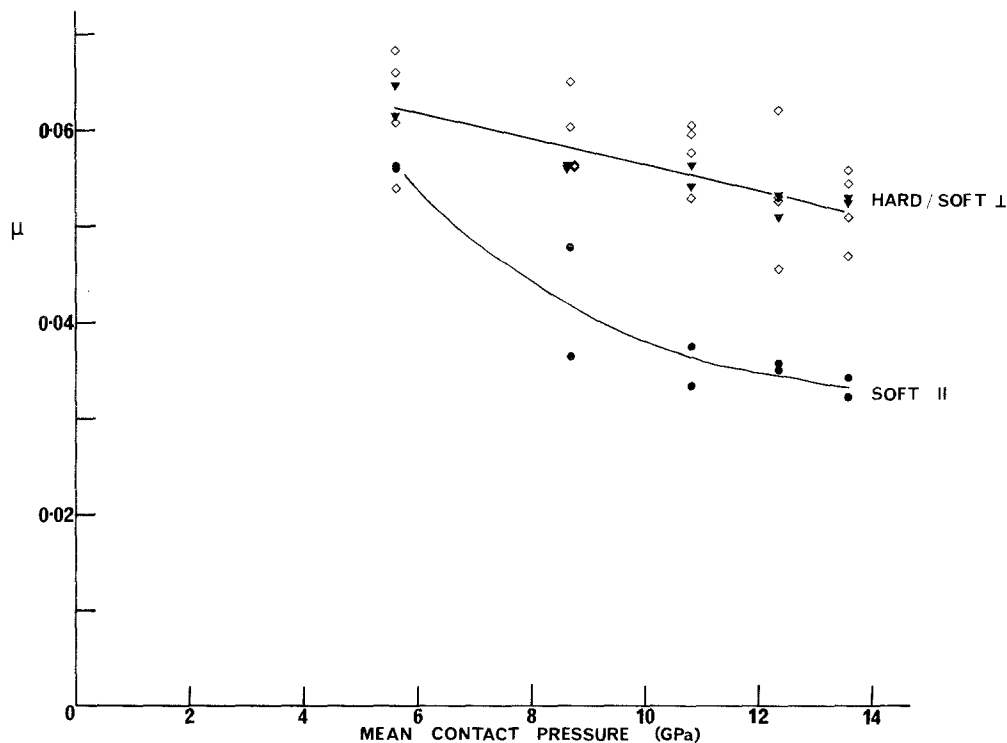


Figure 9 The coefficient of friction of a stylus of radius 370 μm sliding on an (001) surface as a function of mean contact pressure. Solid black symbols refer to $\langle 100 \rangle$ directions. Hard and Soft refer to sliding in $\langle 110 \rangle$ and $\langle 100 \rangle$ directions, respectively, see text. The symbols \perp and \parallel refer to directions perpendicular and parallel to the polish lines which are parallel to $[100]$.

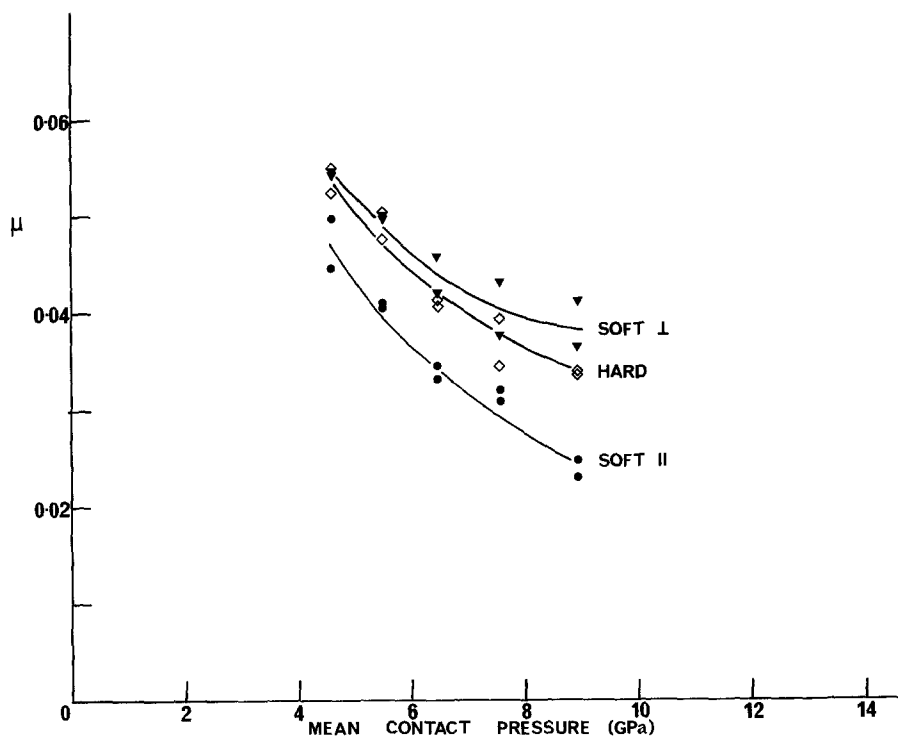


Figure 10 The coefficient of friction of a stylus of radius $490\ \mu\text{m}$ sliding on an (001) surface as a function of mean contact pressure.

by Casey and colleagues [16], and the comparison of damage produced on different tracks. The flat surfaces were polished with 0 to $1\ \mu\text{m}$ powder under standard conditions on a cast-iron wheel, and oriented to the (001) or (011) positions to within $15'$ of arc. After each repolish the surface was inspected in both an optical microscope using the Nomarski technique and using the cathodoluminescence technique in the scanning electron microscope (see Section 5) to ensure that all signs of previous damage had been removed, that the

surface was free of polishing flaws, and that the polishing lines were no more than just visible.

4. The friction of (001) surfaces

The flat (001) faces were polished in the conventional way, with the direction of abrasion and the polishing lines running parallel to one of the cube axes. Measurements of the friction were made in three principal directions, along and perpendicular to the polish lines, and at an angle of 45° to them. (Only one direction was selected at 45° , as all the $\langle 110 \rangle$ directions make similar angles with the polish lines.) Fig. 9 shows results for a $370\ \mu\text{m}$ radius stylus sliding on surface A5c, i.e. repolish c on diamond A5. Each point represents the average of five passes on a previously unused part of the surface. The sliding directions parallel and perpendicular to the polish lines are referred to as Soft_{\parallel} and Soft_{\perp} , these being directions of easy abrasion, and the 45° direction is referred to as Hard as being the hard direction of abrasion. The pressures quoted are the mean pressures calculated from the standard Hertz formula using values of $1.05 \times 10^{12}\ \text{N m}^{-2}$ and 0.2 for the Young's modulus and Poisson's ratio. Despite some scatter on the points, two trends are clearly visible: (a) the coefficient of friction, μ , becomes smaller at the higher pressures, and (b) the friction parallel to the polish lines, μ_{\parallel} , is appreciably less than μ_{\perp} except at the lowest pressure.

Fig. 10 shows another set of measurements made with a $490\ \mu\text{m}$ radius stylus on the repolished surface A5i. All the values of the friction are appreciably lower than those shown in Fig. 7 but the same trends are still observed. The friction decreases with increasing pressure and μ_{\parallel} is appreciably less than the other two coefficients. The differences between the values of the friction in Figs 9 and 10 may possibly arise because of the difference in the radii of the two styli, but this is not large and it seems more likely that the discrepancy arises because of some difference in the surface

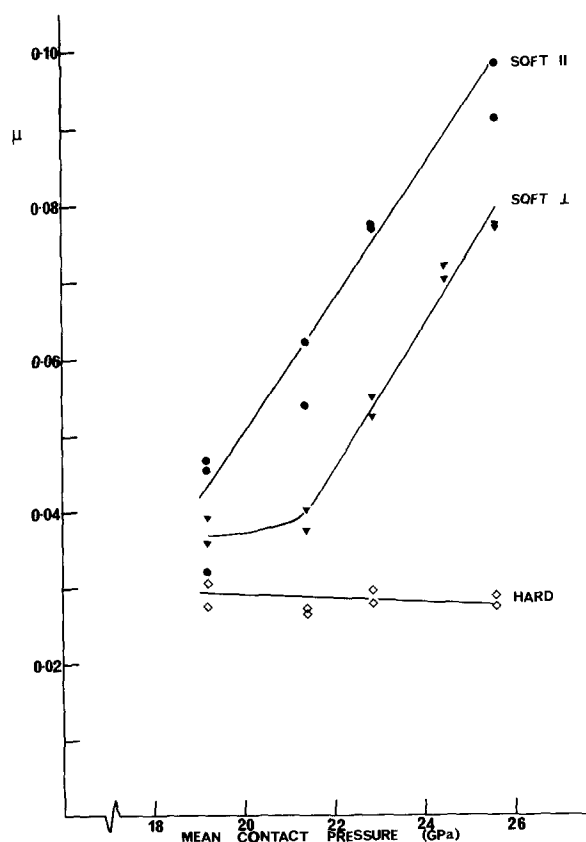


Figure 11 The coefficient of friction of a stylus of radius $60\ \mu\text{m}$ sliding on an (001) surface as a function of mean contact pressure.

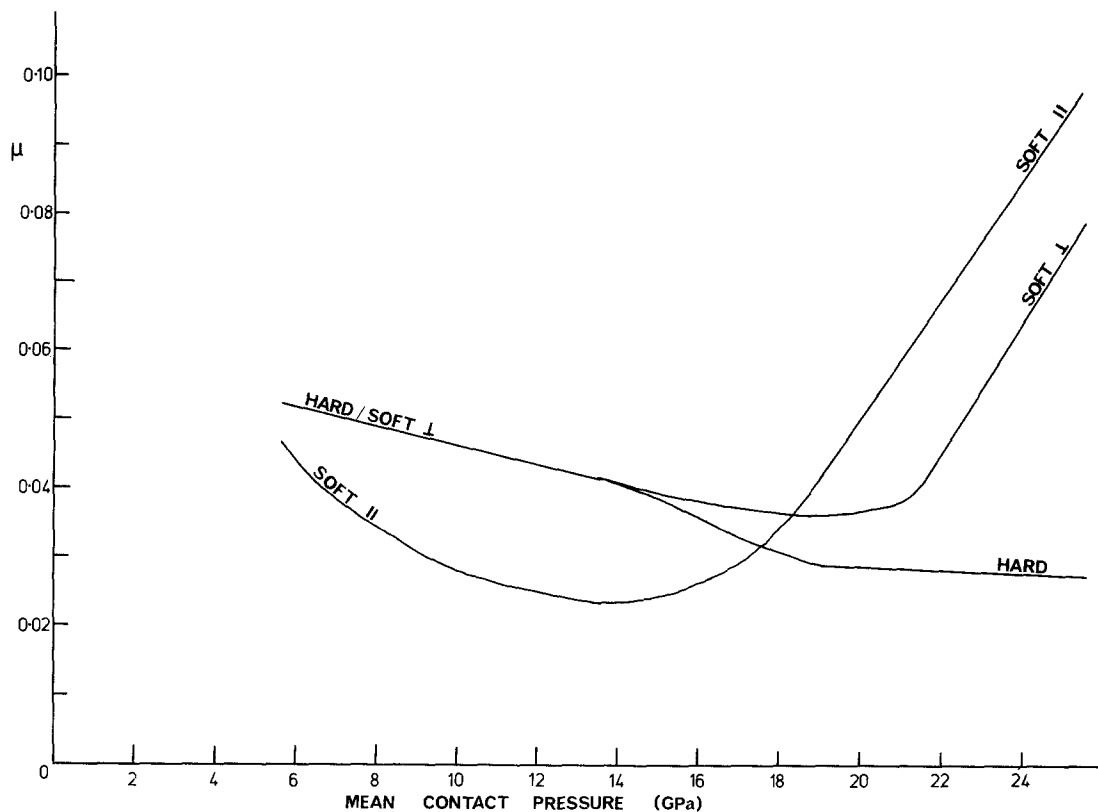


Figure 12 Schematic summary of the experimental results for the coefficient of friction on an (001) face as a function of mean contact pressure.

topography of the styli or surfaces. It is difficult to produce a standard finish on the styli, particularly because a smaller radius involves polishing in directions further from the (011) tangent plane of the stylus, and the quality of the polish depends strongly on the direction of abrasion.

Fig. 11 shows results obtained at higher pressures with a $60 \mu\text{m}$ radius stylus. The dependence on pressure is now different. The coefficients in the soft directions μ_{\parallel} and μ_{\perp} rise steadily with increasing pressure, while in the hard direction, μ_{Hard} , slowly decreases.

Clearly, the results shown in Figs 9, 10 and 11 imply that some cross-over of the curves must occur at intermediate pressures, as shown schematically in Fig. 12. Figs 13 and 14 show results obtained with 100 and $150 \mu\text{m}$ styli, covering the intermediate range of pressures. The change-over from the lower to the higher pressure regime is clearly shown. The two figures also show appreciable differences between the values of the friction at a given pressure, probably due to the difference in the radii and surface polish of the styli. However, we have made 13 sets of measurements

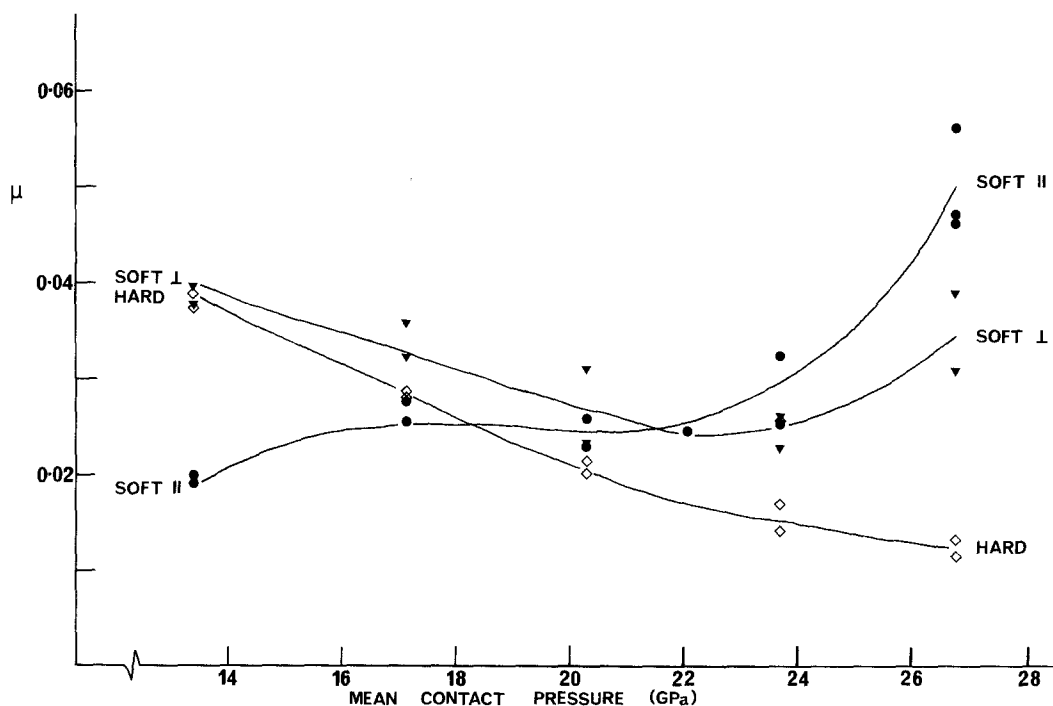


Figure 13 The coefficient of friction of a stylus of radius $100 \mu\text{m}$ sliding on an (001) surface as a function of mean contact pressure.

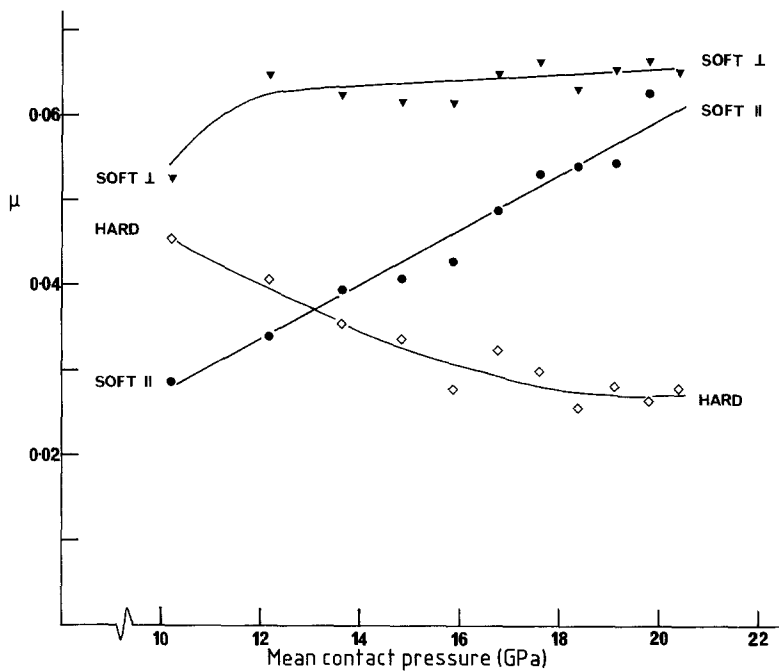


Figure 14 The coefficient of friction of a stylus of radius $150\ \mu\text{m}$ sliding on an (001) surface as a function of mean contact pressure:

at pressures between 4 and 27 GPa, and find that the friction conforms to the general schematic pattern shown in Fig. 12, the differences between the various sets of measurements being similar to those described.

5. Observations of damage

Enomoto and Tabor [1] have stressed the importance of any damage produced on the diamond flat during measurements of the friction. According to these authors the increasing anisotropy of the friction at higher loads (Fig. 3a) arises because of the onset of surface and subsurface damage produced in the flat by the sliding process itself. Therefore, particular care was taken during the present measurements to observe any damage produced in the flat. It is also desirable to monitor any changes in the surface of the stylus, but this is much more difficult because of its curvature. Hence, observations of the styli were limited to checks against any gross damage.

The most obvious damage that may be produced on the flats takes the form of conical cracks, either complete or partial, which appear on the surface as a ring crack or series of ring cracks at pressures above about 25 GPa. These rings are readily observed in the optical microscope using the Nomarski technique, as, for example, in Fig. 15, which shows both complete and incomplete rings. The conical cracks themselves extend downwards and outwards into the surface to a

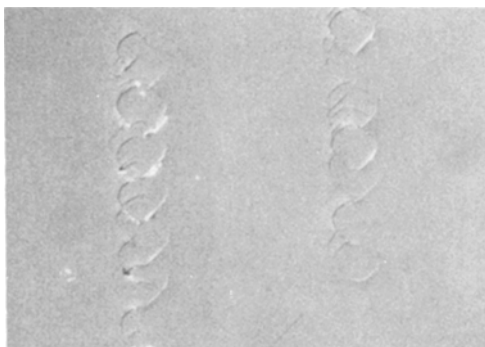


Figure 15 Ring cracks produced by sliding a stylus of radius $145\ \mu\text{m}$ in a $\langle 100 \rangle$ direction on an (001) plane.

depth of the order of the diameter of the ring, and are generally jammed open to some extent by debris produced during the fracture as described by Bell *et al.* [17]. These conical cracks modify the topography of the surface considerably so all our main observations were taken with loads below the limit required to produce such damage.

At lower loads no damage to the flat was visible in the optical microscope, but damage could still be observed when the flat was viewed in the CL mode of the scanning electron microscope. For example, Fig. 16, a micrograph of several friction tracks produced by one, five and ten passes of a stylus over the same paths, shows that the measurements have produced significant darkening of the tracks. As might be expected, the darkening becomes more marked with repeated passes and increasing load, and appears similar to that observed during the progressive fatigue of diamond, the darkening being associated with surface cracking on a fine scale [17]. (The ends of the tracks in Fig. 16 are sometimes darker and somewhat displaced. Later experiments suggest that these effects

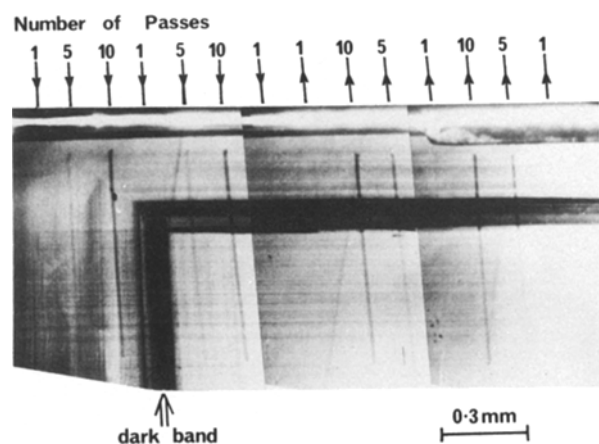


Figure 16 Damage caused by friction tracks viewed in the cathodoluminescent mode of the SEM. The friction tracks are vertical. The pronounced dark right-angle band marks a growth layer in the diamond.

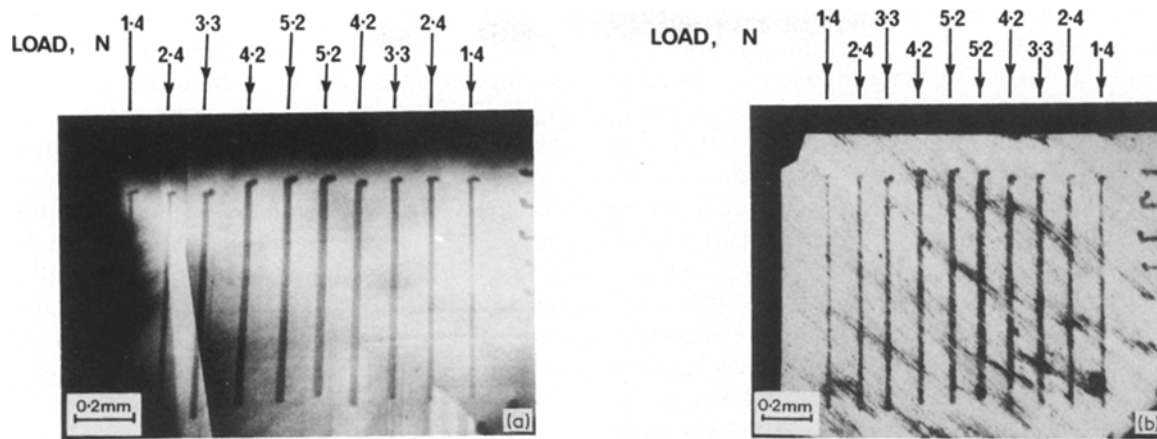


Figure 17 Friction tracks produced by a stylus of radius $340\ \mu\text{m}$. (a) Viewed in the cathodoluminescent mode of the SEM; (b) viewed using the grease technique described in the text.

are due to transitory starting up processes arising from small amounts of play in the bearings carrying the specimens.)

The damage produced in the diamond flat was also revealed by a quite different technique. Thus, the surface of a flat showing damage in CL (Fig. 17a) was gently smeared with a very small amount of grease (Apiezon N vacuum grease). The tracks were then clearly visible in the optical microscope (Fig. 17b). It appears that surface cracking produces a roughening of the surface which results in the preferential retention of the grease.

The diamond flats were carefully examined in the scanning electron microscope after each set of measurements, if necessary by reducing the accelerating voltage in order to concentrate the induced luminescence near the surface. In fact, damage was observed after all the present measurements although, of course, the darkening was greater at the higher loads. No change in the form of the darkening with increasing load could be detected until the abrupt appearance of ring cracks.

6. Discussion

6.1. Dependence of friction on pressure

The form of the present results summarized in Fig. 12 shows that the behaviour of the friction depends strongly on the contact pressure between the surfaces. It appears to be this dependence which is responsible for the apparently differing results obtained by various authors. For example, Hillebrecht [4] used a load of $0.5\ \text{N}$ on a $450\ \mu\text{m}$ stylus, corresponding to a mean pressure of $3.5\ \text{GPa}$, and observed little or no anisotropy in the friction. On increasing the load to produce pressure up to $11\ \text{GPa}$, the value of μ fell by about 10%. Both these results are as would be expected from Fig. 12. On the other hand, Enomoto and Tabor [2] used rounded styli and loads which produced mean pressures of 13.8, 17.4 and $21.9\ \text{GPa}$, and observed anisotropies in the friction which became more marked as the load was increased (Fig. 3a). These results correspond to the right-hand half of Fig. 12. (The mean pressures correspond only approximately, but some difference is to be expected because of possible differences in the orientation and polish of the styli.)

The results obtained with pointed styli are more complex. Bowden and Brookes [12] used diamonds polished to form cones of different vertical angles, while Casey and Wilks [3] used the unpolished tips of natural octahedral diamonds. Consider first the friction given by the 170° cone used by Bowden and Brookes (Fig. 2). The mean pressure due to elastic deformations under an ideal cone is given by

$$p = \frac{E \cot \theta/2}{4(1 - \nu^2)} \quad (1)$$

where E is Young's modulus of diamond, θ the full angle of the cone, and ν Poisson's ratio (see, for example, Johnson [5] p. 114). Substituting in values (taking $\nu = 0.2$) we obtain a pressure of $24\ \text{GPa}$. However, this is certainly an upper limit as the tip can hardly form a geometrically ideal cone. Hence, as the observed friction was almost isotropic, it seems likely that the actual mean pressure corresponded to the central region of Fig. 12.

The position regarding the friction observed with the 120° and 60° cones is more difficult because the assumption that the tips have an ideal conical form is even less realistic. For a 120° cone, Equation 1 gives a mean pressure of $150\ \text{GPa}$, and the tip of the stylus would certainly fracture long before this pressure was reached. In fact, neither Bowden and Brookes nor Casey and Wilks reported any gross cracking of the flats in their experiments, thus setting an upper limit to the pressures of the order of $25\ \text{GPa}$. Thus, the pressure under the 120° and 60° cones probably had magnitudes in the right-hand half of Fig. 12, in which case the higher pressure under the 60° cone would give rise to the higher anisotropy, as observed (Fig. 2).

The measurements of Casey and Wilks, [3] were made using the tips of good quality octahedron diamonds which permitted the accurate crystallographic orientation of the stylus, but the exact shape of the tip was not well defined. However, as the included angle between opposite octahedron faces is 110° we might expect the pressure to be similar to that under the sharper cones used by Bowden and Brookes. This would lead to a pressure corresponding to the right-hand side of Fig. 12 and the friction to show appreciable anisotropy, as observed (Fig. 1a).

Casey and Wilks also found that the coefficient of

friction in both the hard and soft directions showed little or no variation under loads ranging from 3 to 300 gwt (Fig. 3b). This change in load on a spherical tip produces changes in the pressure by a factor of 4.6, but the pressure under a conical tip (Equation 1) is independent of the load. A direct application of this result would explain the observed constancy of the friction but the position must remain open for it is not realistic to use Equation 1 for sharp-angled styli.

To sum up, we note that the present results imply that the pressure between the surfaces is an important parameter in the friction process no matter how the friction forces may arise. At least three different pressure regions are involved. At the lower pressures the coefficient of friction decreases with rising pressure; at the higher pressures the coefficient for sliding in the $\langle 100 \rangle$ directions increases with rising pressure, and at the lowest pressure the friction appears to be independent of the direction of sliding. It follows that the degree of anisotropy is determined largely by the contact pressure.

6.2. Mechanisms of friction

Any account of the mechanisms responsible for the friction force must begin with the nature of the polished surfaces. Diamond shows great resistance to plastic flow and conventionally polished surfaces show no sign of having been smoothed by plastic deformation, as mentioned above. Hence, even well polished surfaces are rough on a scale of the order of 5 nm with asperities outlined mainly by cleavage planes. It follows that if two such surfaces are placed together in close contact, the two sets of asperities will interlock. Any attempt to slide one of the surfaces over the other must be impeded by collisions between these asperities which thus give rise to a friction force. Moreover, continuous relative motion can only occur if the interlocking asperities either ride over each other, push past each other, or fracture. We consider each of these possibilities in turn but first outline some general features of the contact between two rough surfaces.

6.2.1. The contact of rough surfaces

The nature of the contact between two rough elastic surfaces with surface asperities is quite complex. Greenwood [18] has considered the simpler but essentially similar case of a flat plane in contact with a rough surface, the height of the asperities being specified by some distribution function. Two limiting conditions are distinguished, corresponding to high and low loads. Under low loads contact is only made between the tips of the highest asperities, and the area of true contact is a small fraction of the apparent contact area. In the regime of high loads all the asperities have come into contact, and the load on each increases as the total load, W , increases. Rather similar considerations apply for Hertzian type contact [19], though the analysis is now more complicated because the individual microcontacts can no longer be regarded as independent.

The profiles of the polished diamond flats and styli are considerably more complex than the examples

treated above. Three different orders of magnitude are involved in a typical experiment. (i) The bulk depression of the flat is of the order of 1 or 2 μm . (ii) Both surfaces are modulated by polish lines consisting of hills and valleys with vertical height differences varying from perhaps 10 to 100 nm and with a horizontal scale of perhaps 0.5 to 5 μm . (iii) The surfaces are further modulated by the basic polishing process which produces a structure with a vertical and horizontal scale of 5 μm . Note that although the hills and valleys of the polish lines may be clearly visible in the interference microscope their slopes are quite shallow.

Experiments with hard styli resting on hard materials can produce extremely high loadings of the surface. The maximum apparent mean pressure between the surfaces in the present experiments, about 25 GPa, is over 10^8 times greater than that due to a cube of diamond of side 5 mm resting on a flat surface (and close to the value required to produce gross cracking). These pressures will modify the topographies of the polish lines as discussed by McCool [20] who considers the elastic deformation of a system of parallel sinusoidal hills and valleys when compressed elastically by a plane surface. His results, although not directly applicable to the topography of the polish lines, imply that the pressures in the present experiments are of the right order of magnitude to ensure contact over most of the valleys as well as the hill. Therefore, we shall make the assumption that in all the present measurements of the friction, the load was sufficient to cause most of the small-scale asperities on the stylus to be in contact with the flat.

6.2.2. Fracture

Observations of the diamond flat after a measurement of the friction, using both CL and grease techniques, show that some fracture damage is always produced in the surface. Also, small amounts of debris were sometimes detected with the optical microscope, pushed forward by the stylus to the end of the track, perhaps similar material to that observed by Seal [6]. If microfracture is the only mechanism involved in the friction process, then the work done against the friction force must be equal to the work of fracture, that is the additional surface energy of the surfaces created by the fracture. However, estimates of the energy of fracture [2, 21] show that coefficients of friction derived in this way are two orders of magnitude too small.

A particular example of the influence of fracture on the friction has been observed in the present series of measurements using loads near to the critical value for the production of ring cracks. It was sometimes found that ring cracking began some way along the length of a track and that the friction then rose by perhaps 30%. This result might suggest that the work of fracture makes a substantial contribution to the friction, but a further experiment showed otherwise.

The coefficient of friction was measured by five passes in a hard direction using a 65 μm radius stylus with a load of 1.4 N well below the critical load needed to produce ring cracks. Fig. 18 shows the friction observed on the 4th and 5th passes over the same

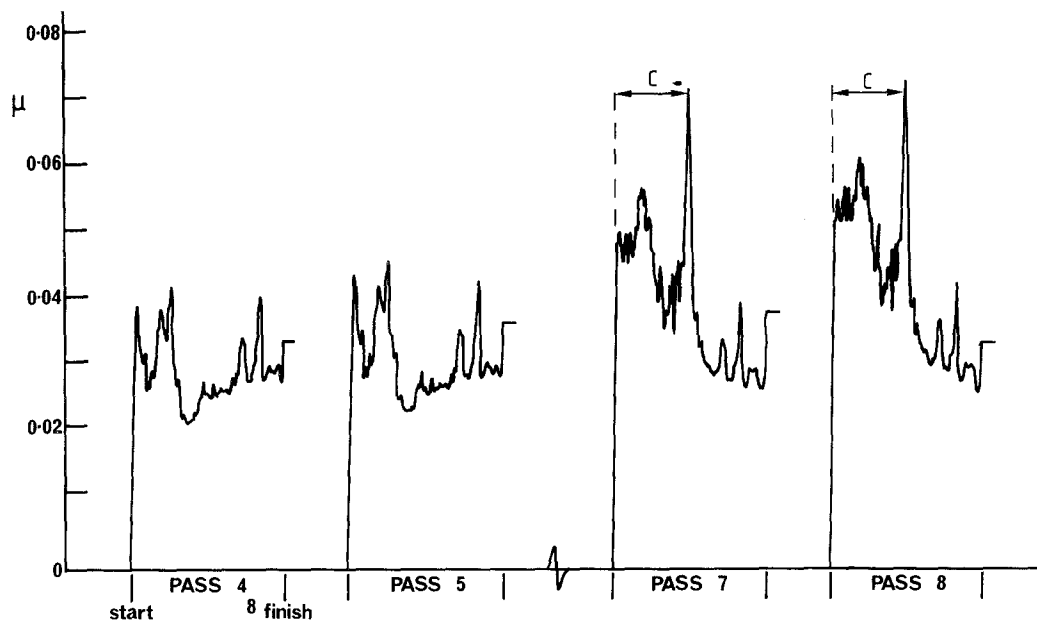


Figure 18 Chart recorder traces from an experiment to investigate the effect of ring cracks on the friction. The arrowed lengths, C, indicate portions of the track on which ring cracks have been produced, see text. Stylus radius $65 \mu\text{m}$; load 1.4 N ; sliding direction $[1 \ 1 \ 0]$.

track. The load was then increased to 10.1 N and a pass made over only the first half of the track thus producing a line of ring cracks. The friction was then remeasured over the whole track using the previous load and the results on passes 7 and 8 are shown in Fig. 18. On the uncracked half of the track the values of μ are similar to those obtained previously but on the cracked part they are appreciably higher. It appears that the production of ring cracks gives rise to a higher friction because of modifications to the topography of the surface, and that the fracture of the surface does not in itself make a major contribution to the friction.

6.2.3. Ratchet mechanism

Consider the position when relative motion of the two surfaces is achieved by the asperities riding over each other. A detailed analysis is quite complicated because each asperity is surrounded by other asperities on the same surface which may or may not be bearing part of the load. However, suppose that as a result of the sliding motion, two asperities, one on the slider and one on the flat, meet and ride over each other. The two surfaces in the region of the asperities are thus forced apart against the load by the friction force. As the sliding continues, contact between the two asperities will be lost and the load taken by other sets of asperities. Because the asperities are rough and irregular, the transference of load to different sets of asperities will be abrupt and irreversible. Hence, some of the work of separation degenerates into heat, and work must be done to maintain the sliding. Variants of this type of friction have been described by Bowden and Tabor [22] and Rabinowitz [23] and described as ratchet or roughness mechanisms.

The coefficient of friction for a ratchet mechanism will depend on the detailed topography of the surfaces including the steepness of the asperities. Taking the asperities to be bounded approximately by cleavage planes, Casey and Wilks [3] show that an irreversible energy loss of about 10% of the stored energy at each

encounter is sufficient to account for the magnitude of the friction. This approach accounts naturally for the dependence of the friction on the method of polishing the diamond surface (Fig. 1), because different methods of polishing produce different topographies with asperities of different shape and overall symmetry. Tabor [24] and Seal [21] have extended this approach by introducing an adhesive force between the interacting asperities. However, it is well established that the friction of diamond on diamond is unchanged by the presence of a light oil, so the assumption of an adhesive force appears somewhat unrealistic. More importantly, none of the above treatments of the ratchet mechanism account for the observed dependence of the friction on pressure, nor take account of the effect of the polish lines.

6.2.4. Elastic losses

The third way in which the asperities on the sliding surfaces can move past each other is by pushing each other aside elastically, a possibility not previously considered. The contact between two such asperities will generally be lost abruptly, leaving them with stored elastic energy which will cause them to vibrate. To make an order of magnitude estimate of this effect we calculate the deflection, δ , of a diamond-like pyramidal asperity bounded by $\{1 \ 1 \ 1\}$ planes when a force, f , parallel to one side of the base is applied on the centre line of a face,

$$\delta = \frac{f}{Ed} \frac{2^{1/2} c(c^2 + 1.2)}{1 - c} = \frac{f}{Ed} \beta \quad (2)$$

where E is the Young modulus, d the length of the side of the base, and c the fraction of the asperity height at which the force is applied. If the force is suddenly released the asperity will vibrate at a frequency at least of the order of $v/2d$ where v is the velocity of longitudinal sound waves, that is a frequency of at least 10^{12} Hertz. The speed of sliding in the present experiments was about $66 \mu\text{m sec}^{-1}$, so taking the distance between

collisions at the lower limit of 5 nm, the time between collisions is $\sim 10^{-4}$ sec. Hence, the asperities would be free to vibrate for $\sim 10^8$ cycles between collisions, sufficient to dissipate most of the elastic energy even though the internal damping in diamond may be very low.

To estimate the effect of the above loss of elastic energy we introduce the basic equation of the friction obtained by considering a unit displacement of the stylus and equating the work done against the friction force with the energy loss in the diamond. Consider the situation in which the stylus is at rest with virtually all its asperities in contact with asperities on the flat. If we now move the slider forward a distance λ equal to the mean distance between the asperities on the stylus, then each stylus asperity will, on average, have made just one collision. Hence the total work done by the stylus over the unit displacement is

$$\mu W = N(1/\lambda)_{\text{stylus}} \varepsilon \quad (3)$$

where W is the load, N the mean number of asperities in contact, and ε the energy loss per collision. Assuming that all the asperities in the apparent area of contact, A , are in real contact, $N \sim A/d^2$. The loss of elastic energy from the pair of asperities involved in each collision

$$\varepsilon = f_{\text{max}} \delta_{\text{max}} = (Ed/\beta)^2 \delta_{\text{max}}^2 \quad (4)$$

Hence, taking $\lambda = d \sim 5$ nm, assuming the point of contact to be half way up the pyramid ($c = 0.5$), and substituting into Equation 3 we find that to obtain a typical value of the friction of 0.05 at 20 GPa pressure requires a value of $\delta/d \sim 0.04$. That is, the loss of stored energy is sufficient to account for the friction if the asperities deflect 0.2 nm at the point of contact without, of course, suffering fracture.

6.3. The dependence of friction on pressure and direction

To estimate the form of friction associated with each mechanism we return to Equation 3 which is equally applicable to both types of mechanism. For the ratchet mechanism we take

$$\varepsilon = \alpha h w \quad (5)$$

where w is the mean load on an asperity, h the distance through which the asperity relaxes before the load is carried on a new set of contacts, and α a fraction of order 0.1. Hence, remembering that $W = Nw$, Equation 3 gives the coefficient of friction associated with the ratchet mechanism as

$$\mu_R \simeq \alpha h/\lambda \quad (6)$$

a result of the right order of magnitude. The dependence of μ_R on pressure will be determined by the behaviour of the relaxation length, h , which is difficult to calculate, but which will certainly decrease as the surface and the asperities move closer together at the higher pressures.

It was shown in Section 6.2.4. that the elastic-loss mechanism gives rise to a coefficient of friction of the right order of magnitude. We now estimate how the coefficient μ_E will vary with the pressure. For a Hertz

indentation with a spherical stylus the area of apparent contact $A \propto p^2$ where p is the overall mean contact pressure. The number of asperities in this area is A/d^2 where $d \sim 5$ nm) and we assume that the majority are in actual contact, hence

$$N \propto p^2$$

The mean load on the asperities

$$w = W/N \propto p^3/p^2 \propto p \quad (7)$$

and the total elastic energy associated with each encounter is

$$\varepsilon_E = \gamma w^2 \propto p^2 \quad (8)$$

where γ is a constant including the elastic moduli. Hence, substituting in Equation 3 we obtain

$$\mu_E \propto p$$

The above estimates show that both the ratchet and elastic-loss mechanisms give coefficients of friction which have the correct order of magnitude and which, respectively, decrease and increase as the mean contact pressure is increased. The models used are of course, approximations for the more complicated real situation where the motion of each asperity, both in and perpendicular to the plane of the surface, is limited by the constraints due to its neighbours. Even so, it appears that a combination of the ratchet and elastic-loss mechanisms is sufficient to account for the general form of the friction in the soft directions shown in Fig. 12.

The marked rise of the coefficient of friction in the soft directions at higher pressures in Fig. 12 is associated with the elastic-loss mechanism. Therefore, it might be expected that the friction in the hard direction would increase with pressure in a similar way, which it clearly does not. However, the elastic loss mechanism will only give a greater friction with increasing pressure provided that the asperities absorb more elastic energy rather than fracture off. In fact, the resolved tensile stresses across the $\{111\}$ cleavage planes due to sliding in the hard direction are about a factor $2^{1/2}$ greater than those produced by sliding in the soft direction. Hence it seems that the friction in the hard direction is limited by the maximum elastic energy which can be stored before fracture.

(The hard direction is, by definition, the most resistant to abrasion and polish, that is to the removal of material. Therefore, it may seem inconsistent to account for the lower friction in this direction by saying that in this direction the asperities are more easily fractured. Note, however, that measurements of the rates of removal of material by abrasion, see for example [7], are made on surfaces which are continuously abraded in the course of the experiment. Hence, apart from an initial start-up condition the surface topography is always characteristic of the direction of polishing. In fact, it is the difference of surface topography produced by polishing in $[100]$ and $[110]$ directions that is responsible for the different abrasion rates. However, all the present friction measurements were made on a surface which had been polished in a soft direction, with surface topography

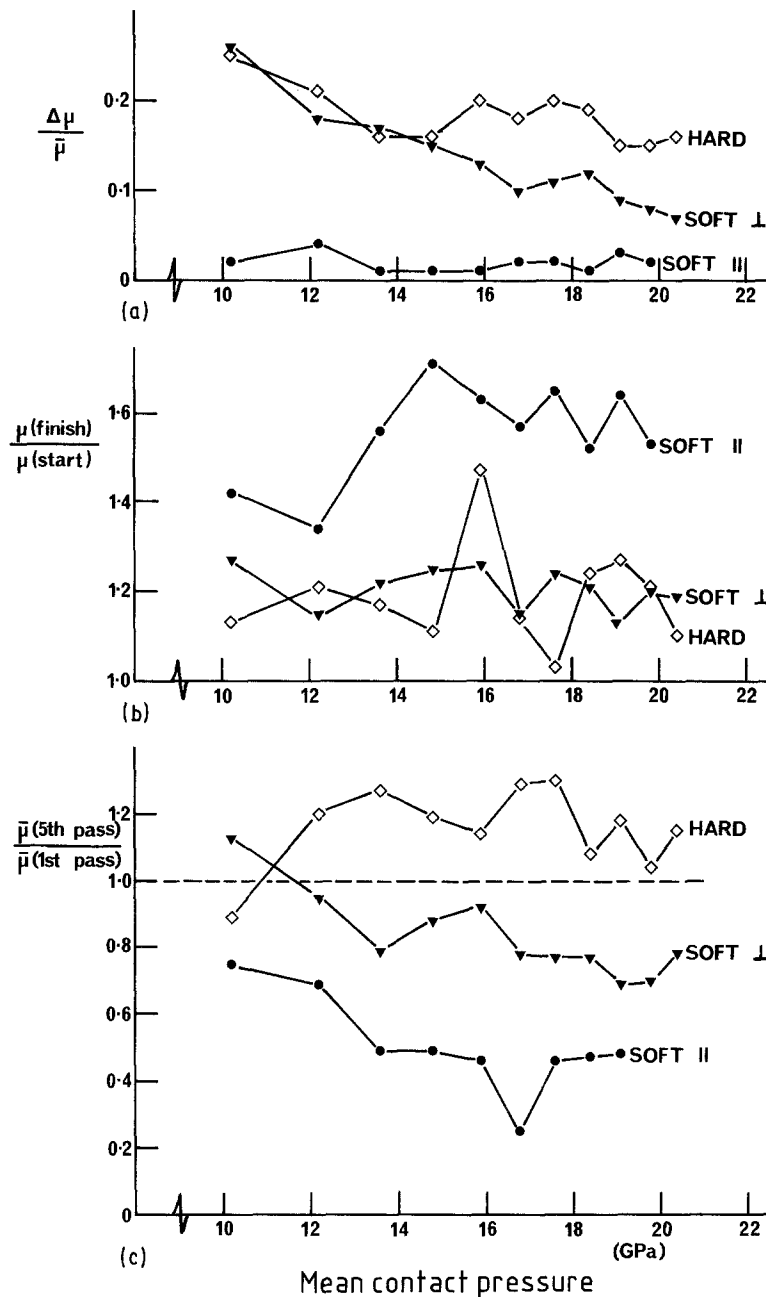


Figure 19 Variations in the coefficient of friction during measurements with a stylus of radius $150\ \mu\text{m}$ sliding on an (001) surface, as a function of contact pressure, see text.

characteristic of this direction, and on this surface the asperities will be more easily removed by attack in the [1 0 0] direction. We recall that Seal [13] observed the coefficient of friction for sliding in the hard [1 1 0] direction over a large number of passes on the same track, and found that after about 100 passes the friction rose by a factor of about 2. Quite possibly this rise was the result of the stylus creating a surface polish characteristic of the hard direction, with a corresponding increase in the forces required to fracture the asperities.)

We now consider the differences in the friction for sliding in different directions at lower pressures, a difference which is most marked in the range below 14 GPa (Fig. 12). This is the region where the ratchet mechanism predominates, so at first sight it might seem that sliding across the hills and valleys of the polishing lines would lead to a greater dissipation of energy. However, as discussed above, the pressures involved are probably sufficient to bring both hills and valleys into contact, so the roughness responsible for the irreversible losses will be on a scale of 5 nm rather

than the 50 nm depths of the valleys. It therefore seems likely that the polishing process has produced a structure even on the very fine 5 nm scale which tends to ease the passage of asperities sliding parallel to the direction of polish. Hence, the friction is least in the direction of polish.

Thus the ratchet and elastic loss mechanisms account reasonably well for the form of the results, although some details remain. For example, it is not clear why in the high-pressure regime the friction is somewhat greater for sliding parallel to the polish lines. Nor is it clear why the coefficients of friction in all three directions tend to the same value at the lowest pressure, although in this case the number of contacts between asperities may be so reduced that statistical variations in their form and distribution tend to blur our directional effects.

6.5. Variation of friction during the measurements

The values of the friction discussed above are those shown in Figs 9 to 14 which are averages taken over

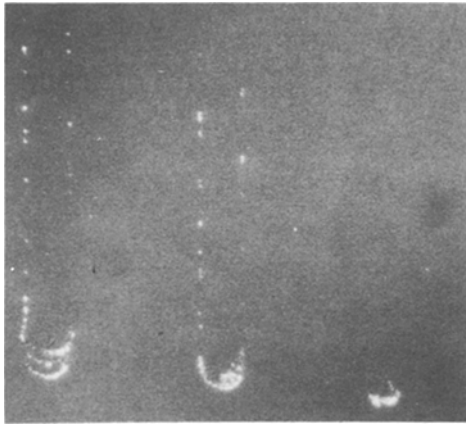


Figure 20 Nomarski optical micrograph showing debris at the end of tracks produced by a stylus of radius $181\ \mu\text{m}$ sliding on an (001) surface in a $\langle 100 \rangle$ direction perpendicular to the polish lines.

five passes on the same track. However, the value of the friction force varies appreciably during each pass as shown in Fig. 6, and may also vary from pass to pass on the same track. At least three types of variation may be observed. First, fluctuations of the order of 10% of the mean which appear random but are observed on subsequent passes over the same track. Second, a tendency for the friction force to rise along one pass. Third, progressive changes in the friction over successive passes on the same track.

Fig. 19 summarizes observations from one set of measurements as a function of the pressure. Some of the details are quite complex but several salient features can be understood in the light of the above treatment. Fig. 19a shows the mean amplitude, $\Delta\mu$, of the fluctuations which are presumably associated with irregularities in the surfaces. As might be expected, the irregularities are less marked when sliding takes place parallel to the polish lines. The amplitude of the fluctuations tends to decrease with increasing pressure probably because of the increasing number of contacts between asperities and a corresponding reduction in statistical variation.

Fig. 19b shows the increase of the friction over the length of a pass as the ratio $\mu(\text{finish})/\mu(\text{start})$. If successive passes of the stylus are made on the same track, it is generally found that similar values of this ratio are again observed. It follows that the rise is not due to wear on either the flat or stylus. At least two processes contribute to this rise. Because the specimen flat moves on the arc of a circle, the surface though horizontal at the start of a pass has tilted through about $20'$ of arc by the end of the measurements, so increasing the coefficient of friction by $\tan^{-1}(20')$, that is by the order of 10%.

A second effect is sometimes responsible for a much larger rise, as in the results for the Soft_{\parallel} direction in Fig. 19b. This rise is often accompanied by a build-up of some material, presumably debris, in front of the stylus, which may be detected in the optical microscope (Fig. 20) and recalls the perhaps similar "waxy deposit" seen by Seal [13]. A build-up of debris in front of the stylus during a pass will increase the force required to move the stylus, and this debris is most likely to build up when pushed along the grooves of the polishing lines.

The effect of debris is confirmed by the experiment of Fig. 21. Four successive passes of the stylus were made in a $\langle 100 \rangle$ direction perpendicular to the polish lines, and each time the friction was observed to rise by almost 50% over the length of the path. Three further passes were made on the same track, then four more passes when the stylus was stopped half-way along the track, lifted clear of the surface, advanced about $100\ \mu\text{m}$, lowered into contact again, and the pass continued. Lifting and advancing the stylus reduced the friction (Fig. 21) but the rise started afresh as the stylus moved on over the second half of the track. Presumably the build-up of debris from the first half of the track was left behind when the stylus was raised. Finally, another four passes were made over the whole track. The first of these, pass 9, showed a large peak where the stylus had previously been lifted from the surface. This peak gradually disappeared over the next three passes, see pass 12, and

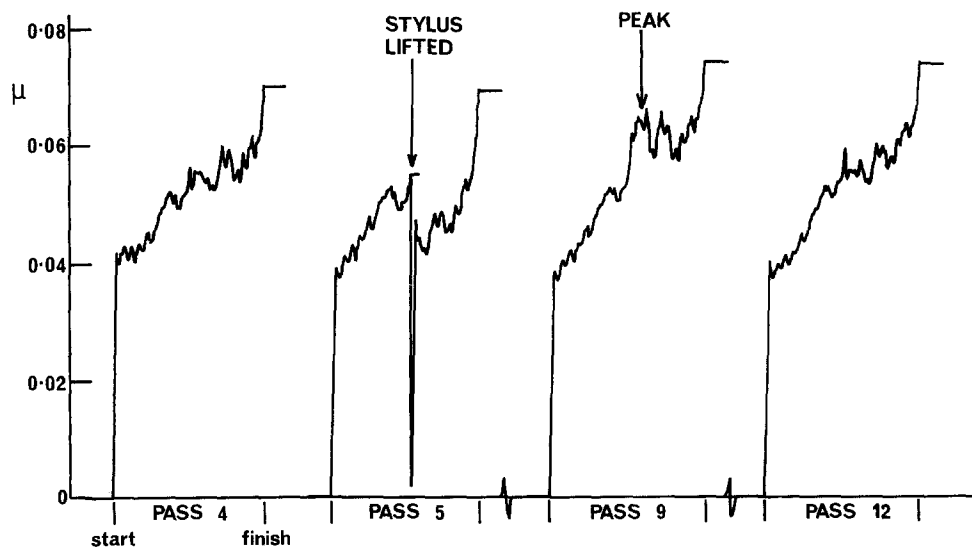


Figure 21 Chart recorder traces from an experiment to investigate the rise in friction over the length of a pass, see text. Radius of stylus $170\ \mu\text{m}$; load $1.4\ \text{N}$; sliding direction parallel to the polish lines.

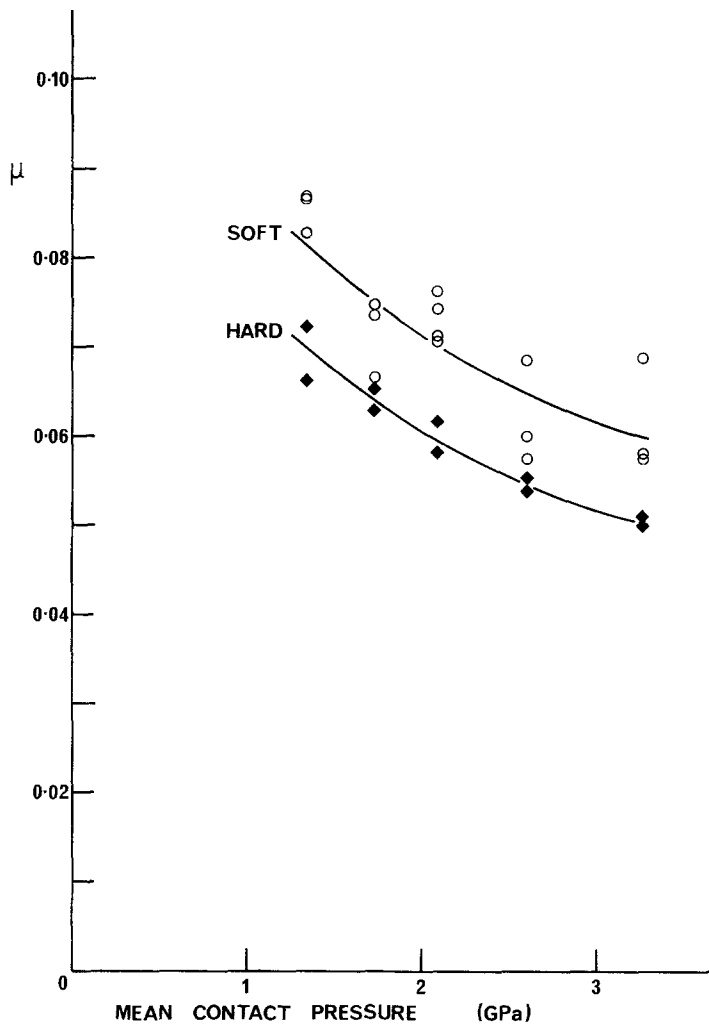


Figure 22 The coefficient of friction of a stylus of radius $3130 \mu\text{m}$ sliding on an (011) surface as a function of mean contact pressure. Soft and Hard refer to sliding in the [100] and [011] directions, respectively, see text.

must have been due to the debris left by the interruption of the earlier passes.

Fig. 19c summarizes some particularly marked changes of the friction during successive passes over the same track. Presumably the passage of the stylus modifies the track and hence the value of the friction, as observed also by Seal [13] and Casey [14]. One might suppose that the action of the stylus would smooth the track and reduce the friction as is the case in Fig. 19c for sliding in the soft directions. In contrast, however, the same figure shows that repeated passes in the hard direction lead to a greater friction. As discussed above, the friction in the hard direction at the relatively high pressures concerned is probably limited by the fracture of asperities. It may be that during the initial passes particularly weak asperities are removed preferentially so that the friction is higher on subsequent passes.

7. The friction of (011) surfaces

All the experiments discussed so far have concerned measurements on an (001) face but the mechanisms used to explain these results appear to apply to the friction of other crystallographic faces. Therefore, it seemed desirable to make further measurements in which the flat (001) surface was replaced by another surface of a different crystallographic orientation. An (011) face was chosen as this orientation may be readily polished to give a smooth surface, and the abrasion resistance depends considerably on the direc-

tion of abrasion, this indicating some anisotropy in the topography of the surface.

Measurements were made in a similar way to those on the cube face except that passes were made in only two directions because of the lower symmetry of the (011) face. The soft or easy directions of polish and abrasion are parallel and anti-parallel to the [100] axis, while the hard directions are parallel and anti-parallel to the $[01\bar{1}]$ axis. Thus, an (011) face polished in the normal way in the soft direction presents two principal directions for the friction measurements, the soft direction parallel to the polish lines and the hard direction perpendicular to the polish lines, and measurements were made in these two directions.

Sliding in the soft direction under pressures of more than about 8 GPa produced ring cracks but as in the previous experiments measurements were only made in conditions free of ring cracking. It was, however, found useful to extend the pressure range to somewhat lower pressures by using a stylus of larger radius. Figs 22 to 24 shows the results obtained with three styli covering the ranges 1 to 3, 4 to 9, and 6 to 10 GPa. As previously, there are differences in the absolute values of the friction measured with different styli at the same pressure, but these are relatively small. We therefore combine the three sets of results to obtain a schematic diagram showing the pressure dependence over the whole pressure range (Fig. 25).

The form of the curves in Fig. 25 recall the results for the (001) surface summarized in Fig. 12 although

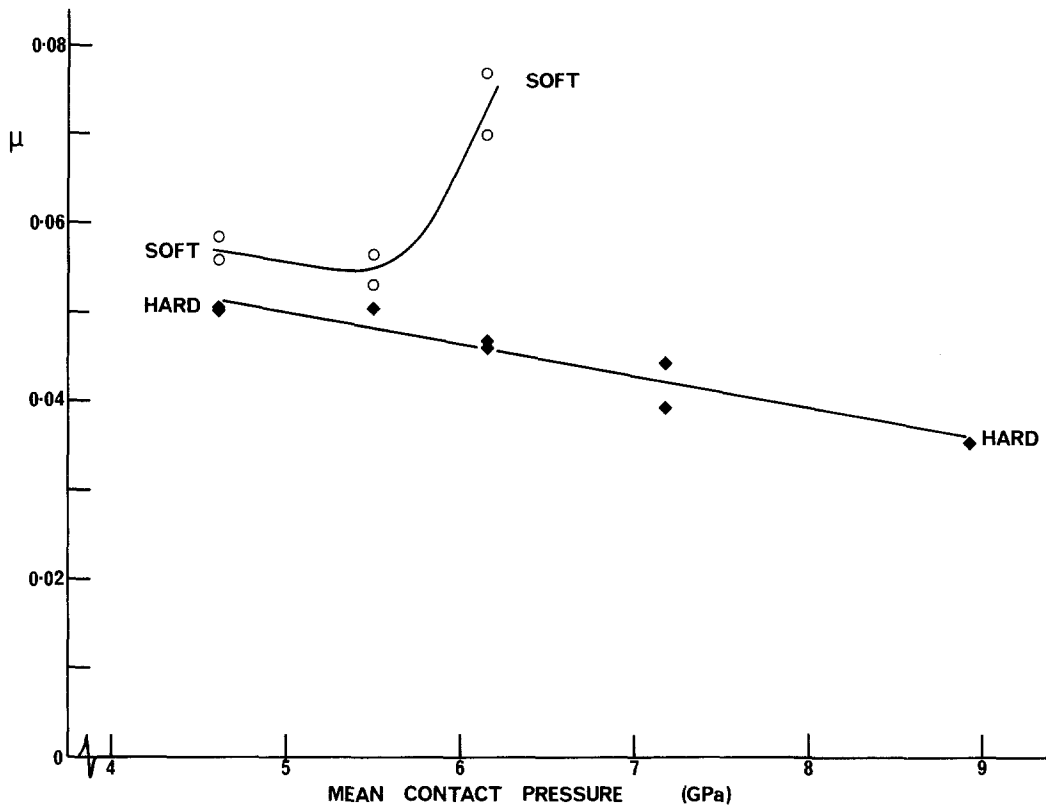


Figure 23 The coefficient of friction of a stylus of radius $490\ \mu\text{m}$ sliding on an (011) surface as a function of mean contact pressure.

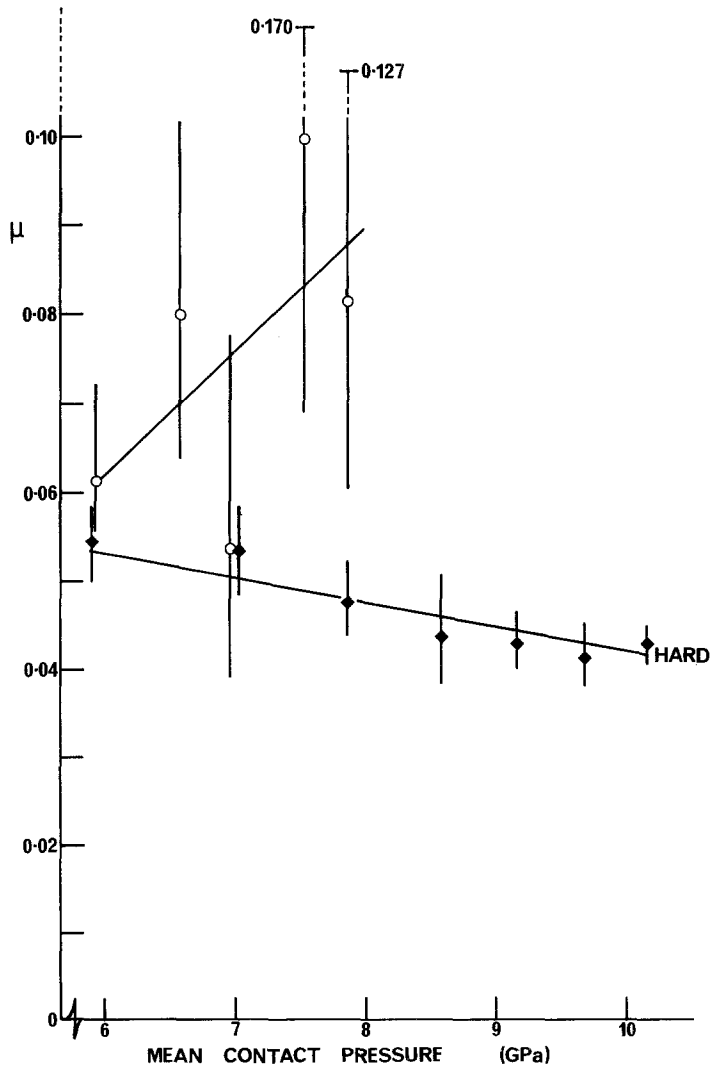


Figure 24 The coefficient of friction of a stylus of radius $340\ \mu\text{m}$ sliding on an (011) surface as a function of mean contact pressure.

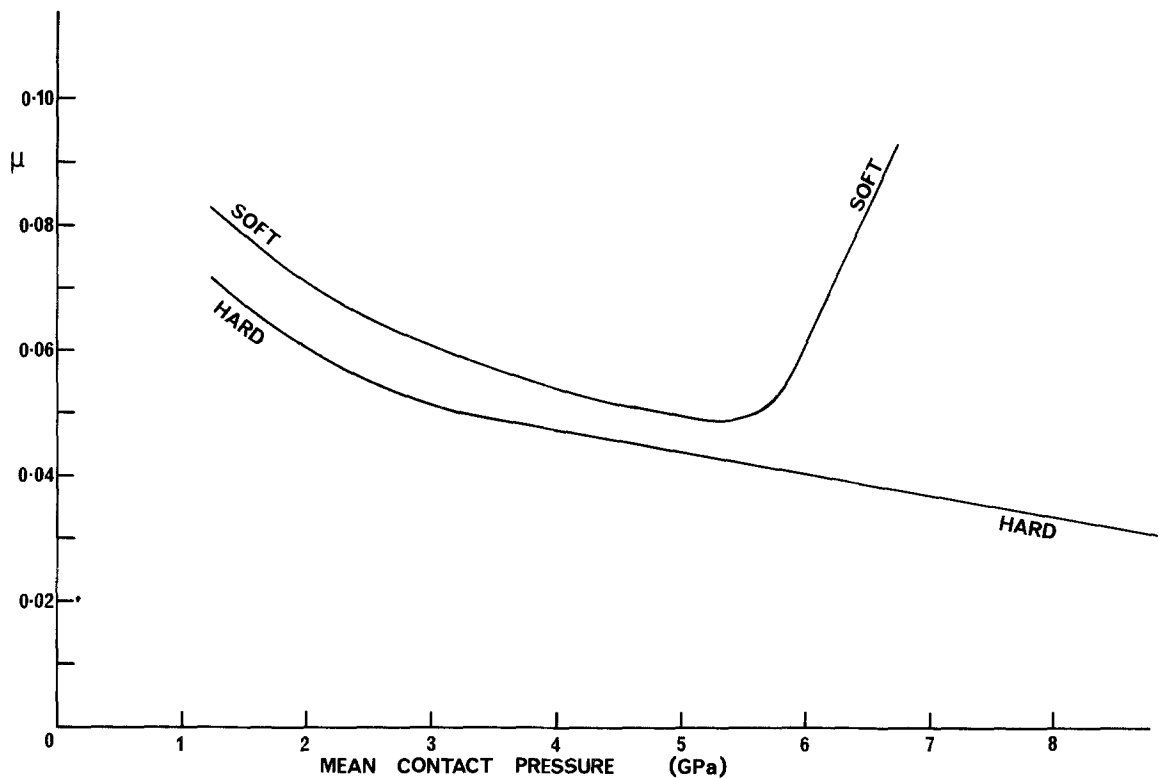


Figure 25 Schematic summary of the experimental results for the coefficient of friction on an (011) face as a function of mean contact pressure.

the absolute values of the pressure are different. In particular, the coefficient of friction in the soft direction first falls with rising pressure and then rises, while the coefficient in the hard direction falls with rising pressure and continues to fall although more slowly at the higher pressures. Thus, the behaviour of the friction is generally similar to that on the (001) face, although some points call for further comment.

The minima in Figs 12 and 25 come about as the result of the superposition of two different processes, the ratchet mechanism and the elastic loss mechanism. Hence the position of the minimum will be determined by the relative magnitudes of the friction arising from each process. The absolute value of each component will be determined *inter alia* by the detailed topographies of both the polished stylus and the polished flat which are not well specified. However, electron microscope studies show that the topography of a polished (011) surface is appreciably different from that of a polished (001) surface [9]. Thus, we expect the components of the friction to differ from one face to another, with a resulting shift in the position of the minimum.

Although an exact calculation of the various components of friction is hardly possible, the resolved tensile stress across the cleavage planes cutting a polished (011) surface will be about $2^{1/2}x$ greater for sliding in the $[01\bar{1}]$ (hard) direction than in the $[100]$ direction. Hence, the asperities will fracture more readily when the stylus moves in the $[01\bar{1}]$ direction. Thus, following the discussion of the elastic loss mechanism in Section 6.4, the friction in the hard direction on the (011) face in the high pressure regime may again be limited to some approximately constant value, as is observed.

Finally, we consider the small but marked difference between the friction in the hard and soft directions in the low-pressure regime. On the (001) face the friction was greater when the stylus slid across, rather than along, the polish lines. On the (011) face, the coefficient of friction for sliding in a direction perpendicular to the polish lines is lower than for the direction parallel to the lines. However, the two sets of results are not directly comparable. On the (001) face the directions parallel and perpendicular to the polish lines are both $\langle 100 \rangle$, whereas on the (011) face the parallel direction is $[100]$ and the hard direction $[01\bar{1}]$. Hence the asperities on the (011) face present different geometries of the stylus in the two directions of motion. In fact, motion in the hard direction offers a greater possibility of a stylus moving around the sides of the asperities rather than being forced to move over them. This effect will reduce the energy loss in the ratchet mechanism and appears to be sufficient to offset any additional friction due to motion across the polishing lines.

8. Conclusions

The friction of diamond sliding on diamond is a complex phenomenon depending on the crystallographic orientation of the diamonds and the quality of their surface polish, the latter being particularly difficult to assess. The present experiments were designed to keep other parameters constant and to vary the pressure between the sliding contacts. The results show that the friction depends substantially on the apparent pressure between the surfaces. On both (001) and (011) faces the coefficient of friction in the $\langle 100 \rangle$ directions falls with increasing pressure, passes through a minimum and then rises. This behaviour suggests that

at least two different mechanisms of friction are involved. The summary of the measurements given by Fig. 12 shows that the friction in one direction may be greater, equal to, or less than the friction in another depending on the pressure between the surfaces, a result which accounts for apparently contradictory results in earlier experiments.

Examination of the flat surfaces in the CL mode of the scanning electron microscope shows that damage was always produced by a friction measurement under even the lowest pressures. The damage appears similar to that observed in fatigue measurements [17] and probably consists of an assembly of fine cracks. This damage was often accompanied by a visible collection of debris at the end of a friction track, and could also be made visible by its preferential attraction of a thin film of grease. These observations all confirm the very brittle nature of the diamond surface.

Any account of the friction of diamond on diamond must start from the well-nigh unique nature of the polished diamond surface. Even apparently smooth and well-polished surfaces are rough and jagged on a microscopic scale, as shown by measurements of the abrasion resistance and friction and by the inspection of high-resolution replicas in the electron microscope [9]. Given this type of surface, it is inevitable that the relative motion of the pair of surfaces in a friction experiment will be resisted by the interlocking of the asperities. Thus, if two surfaces in contact are forced past each other, there are only four possibilities for the asperities. They must either break off, plastically deform, push past each other or ride over each other. Plastic deformation under the conditions of the experiments is ruled out by the nature of diamond. Fracture may occur but cannot account for the magnitude of the friction. The other two possibilities, pushing past and riding over, lead to losses associated with what we have called the elastic and ratchet mechanisms of friction.

The two loss processes of the elastic and ratchet mechanisms must certainly occur during the sliding of diamond on diamond. It is hardly possible to make an exact estimate of the expected coefficients of friction, but the above estimates show that these two mechanisms alone may account for the general form of the friction, including its dependence on the pressure between the surfaces. Further studies of the detailed topography of diamond surfaces would be helpful in clarifying some of the details of the present treatment, for example the role played by the polishing lines in the low-pressure regime, and the decrease of the ratchet-type friction with increasing pressure. Finally, we note that though some adhesive force may be pres-

ent between the asperities despite the presence of the air film, as proposed by Tabor [24] and Seal [21], there appears no need to invoke such a force to account for the experimental results.

Acknowledgements

We thank De Beers Industrial Diamond Division for their support of this work and for a research studentship for one of us (BS).

References

1. Y. ENOMOTO and D. TABOR, *Nature* **283** (1980) 51.
2. *Idem*, *Proc. Roy. Soc. A* **373** (1981) 405.
3. M. CASEY and J. WILKS, *J. Phys. D Appl. Phys.* **6** (1973) 1772.
4. F. U. HILLEBRECHT, MSc thesis, Oxford University (1981).
5. F. P. BOWDEN and A. E. HANWELL, *Proc. Roy. Soc. A* **295** (1966) 233.
6. M. SEAL *ibid.* **248** (1958) 379.
7. E. M. WILKS and J. WILKS, *J. Phys. D Appl. Phys.* **5** (1972) 1902.
8. J. WILKS, *Nature* **243** (1973) 15.
9. A. G. THORNTON and J. WILKS, *J. Phys. D Appl. Phys.* **9** (1976) 27.
10. A. G. THORNTON and J. WILKS, in "Diamond Research 1974", supplement to Industrial Diamond Review, (DeBeer Industrial Diamond Division, Ascot, 1974) p. 39.
11. A. G. THORNTON, (1977) Personal communication.
12. F. P. BOWDEN and C. A. BROOKES, *Proc. Roy. Soc. A* **295** (1966) 244.
13. M. SEAL, in "The Science and Technology of Industrial Diamonds", Vol. 1, edited by J. Burls (Industrial Diamond Information Bureau, London, 1967) p. 145.
14. M. CASEY, D Phil thesis, Oxford University.
15. K. L. JOHNSON, in "Contact Mechanics" (Cambridge University Press, 1985).
16. M. CASEY, A. G. LEWIS, A. G. THORNTON and J. WILKS, *J. Phys. D Appl. Phys.* **10** (1977) 1877.
17. J. G. BELL, M. E. C. STUVINGA, A. G. THORNTON and J. WILKS, *ibid.* **10** (1977) 1379.
18. J. A. GREENWOOD, *J. Lubric. Tech. Trans. ASME* **89** (1967) 81.
19. J. A. GREENWOOD and J. H. TRIPP, *J. Appl. Mech. Trans. ASME* **34** (1967) 153.
20. J. I. MCCOOL, *Wear* **86** (1983) 105.
21. M. SEAL, *Phil. Mag.* **A43** (1981) 587.
22. F. P. BOWDEN and D. TABOR, in "The Friction and Lubrication of Solids, Part I" (Clarendon, Oxford, 1950) p.171.
23. E. RABINOWICZ, in "The Friction and Wear of Materials (Wiley, New York, 1965) p. 675.
24. D. TABOR, in "The Properties of Diamond", edited by J. E. Field (Academic, London, 1979) p. 325.

Received 20 August
and accepted 1 December 1987